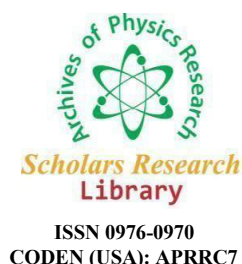




Scholars Research Library

Archives of Physics Research, 2019, 10(2): 3-8  
(<http://scholarsresearchlibrary.com/archive.html>)



ISSN 0976-0970  
CODEN (USA): APRRC7

## Theoretical Investigation of the Influence of Susceptibility Difference between the Central Core-atoms of Water and the Surrounding Cells on the Splitting of Water Peaks

Tariq Ali<sup>1</sup>, M. Imtiaz Khan<sup>1\*</sup>, Hazrat Ali<sup>1</sup>, M. Zubair<sup>2</sup>

<sup>1</sup>Department of Physics, Abbottabad University of Science and Technology Havelian, Khyber Pakhtunkhwa, Pakistan

<sup>2</sup>College of Materials Science and Engineering, Key Laboratory of Advance Functional Material, Ministry of Education, Beijing University of Technology, Beijing, 1000124, China

\*Corresponding Author: M. Imtiaz Khan, Department of Physics, Abbottabad University of Science and Technology Havelian, Khyber Pakhtunkhwa, Pakistan, E-mail: [muimtiazkhan@gmail.com](mailto:muimtiazkhan@gmail.com)

---

### ABSTRACT

Previous nuclear magnetic resonance (NMR) studies by Chen et al. (*Magnetic Resonance in Medicine* 50, 515-521 (2003)) have demonstrated that the water peaks in NMR experiments have been split into two resolved peaks at magic angle spinning due to the isotropic susceptibility shift. The first peak of spectrum rises due to a central core-atoms of water and the second peak is due to tightly packed cells surrounding the water. We present theoretically the atomic model which is based on three-level  $A$ -type and three level  $\Xi$ -cascade atomic configurations of the cell to study the dependency of susceptibility difference on the splitting of water peaks. In addition, we study the effect of the strength of the magnetic field, the magic spinning angle, the electric field, and detunings on the splitting of water peaks.

**Keywords:** Splitting of water peaks, Magic angle spinning, Nuclear magnetic resonance.

---

### INTRODUCTION

High-resolution magic angle spinning (HR-MAS) nuclear magnetic resonance has become a reference tool in many disciplines like chemistry, food sciences and materials science to study heterogeneous samples having liquid-like dynamics which allows us to obtain highly resolved spectra in these samples [1]. In heterogeneous samples, phenomena like the anisotropic chemical shift, the susceptibility variations, and the dipolar interaction can be measured at different MAS by keeping the static field direction [2-5]. Studies of diverse materials, for instance, the inorganic solids and macro-molecular crystals have been done to access at the atomic-level in solid-state NMR. Several techniques have been developed for getting the resolved spectra of samples like the intact organs and living animals at the slower spinning speeds [6]. For example, side-band suppression by the rotor in NMR has been used to study the slower spinning studies of excised human tissues [7,8]. In addition, the magic angle turning (MAT) spectra of metabolites in organs and tissues have been obtained for both living mice and excised tissues [6,7].

Chen et al. [9] reported proton NMR spectra of freshly isolated human skeletal muscle samples. Here, the  $^1\text{H}$  signals of creatine and phosphocreatine with distinct chemical shifts have been resolved and well separated by employing the HR-MAS technique to spin the sample rapidly at  $54.7^\circ$  while keeping the static magnetic field throughout the experiment. It is reported that the creatine resonances split into two peaks and the phosphocreatine resonance remains a singlet, respectively. The creatine has a resonance with the broader linewidth which is motion-restricted [9].

In recent years, the studies of transportation and the exchange of water in different animal tissues have grown to become an interesting area of research. The splitting of water resonance into two peaks has arisen due to the isotropic susceptibility shift under the normal physical conditions of the liquid. The sharp peak is originated due to the free-

water cell and the broader peak arose due to the water pool of the dense-layer of the outer cell [5,6,10]. Philp et al. [11] have questioned the origin of the split water peaks by executing variable angle spinning (VAS) NMR experiments and have introduced corrections to the mathematical model of the isotopic shift.

In this article, we study the splitting of water peaks in a human cell where each cell consists of a water molecule and red blood cell. We investigate the effect of the spinning magic angle, the strength of the magnetic field, electric field, and detunings on the splitting of water peaks in the cell. We show the enhancement of the splitting peaks of the water by including all the mentioned effects.

MODEL

We study the light pulse excitation inside a medium where each molecule of the medium consists of  $\Lambda$ -type atomic configuration of water and  $\Xi$ -type of red blood cell. The energy eigen level configuration for water atom and the red blood cell with supposing atom-field interactions are shown in Figure 1a and 1b, respectively. First, we consider a realistic  $\Lambda$ -type atomic system of water atom having three energy levels  $|1\rangle$ ,  $|2\rangle$  and  $|3\rangle$ . A weak probe field  $E_p$  is employed between level  $|1\rangle$  and  $|2\rangle$  with Rabi frequency  $\Omega_p$ . In the same way, a strong driving field  $E_1$  is incorporated between energy eigen state  $|2\rangle$  and  $|3\rangle$  with Rabi frequency  $\Omega_1$ . Here,  $\gamma_1$  is the spontaneous decay rate of the upper eigen state between  $|1\rangle$  and  $|2\rangle$   $\Gamma_1$  is the decay rate between levels  $|2\rangle$  and  $|3\rangle$ , respectively. We consider three-level cascade  $\Xi$ -type configuration of red blood cell having energy levels  $|a\rangle$ ,  $|b\rangle$  and  $|c\rangle$ . The weak probe field  $E_p$  is applied between  $|a\rangle$  and  $|b\rangle$  the intense laser field  $E_2$  is applied between  $|b\rangle$  and  $|c\rangle$ . The  $\gamma_2$  is the spontaneous decay rate between  $|b\rangle$  and  $|a\rangle$   $\Gamma_2$  is the decay rate between levels  $|c\rangle$  and  $|a\rangle$ , respectively.

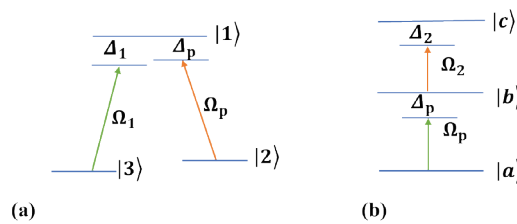


Figure 1: (a) Cartoon of the atomic medium; (b) schematics of the atom-field interaction

To calculate the linear optical susceptibility corresponding to the probe light  $E_p$ , we follow the same approach as in [12-15]. The interaction picture Hamiltonians for these atomic-field systems, under the dipole approximation, can, therefore, be written as:

$$H_w = \frac{-\hbar}{2} (\Omega_p e^{-i\Delta_p t} |1\rangle\langle 2| + \Omega_1 e^{-i\Delta_1 t} |1\rangle\langle 3|) + H.C \tag{1}$$

$$H_c = \frac{-\hbar}{2} (\Omega_p e^{-i\Delta_p t} |b\rangle\langle a| + \Omega_2 e^{-i\Delta_2 t} |c\rangle\langle b|) + H.C \tag{2}$$

where the equation (1) and equation (2) presents the Hamiltonian for water-atom and red blood cell, respectively. Here  $\Delta_p$ ,  $\Delta_1$ , and  $\Delta_2$  are the detunings of the probe and driving fields, respectively. Another assumption is that the driving fields are much stronger than the probe field i.e.,  $|\Omega_1|$  and  $|\Omega_2| \gg |\Omega_p|$ . Here, the rate equations for both cases are given by

$$\rho_{12} = (i\Delta_p - \gamma_1) \rho_{12} + i\Omega_p (\rho_{11} - \rho_{22}) + i\Omega_1 \rho_{32}, \tag{3}$$

$$\rho_{32} = (i\Delta_p - i\Delta_1 - \Gamma_1) \rho_{32} + i\Omega_1 \rho_{12} + i\Omega_p \rho_{31}, \tag{4}$$

$$\rho_{ba} = (i\Delta_p - \gamma_2) \rho_{ba} + i\Omega_p (\rho_{aa} - \rho_{bb}) + i\Omega_2 \rho_{ca}, \tag{5}$$

$$\rho_{ca} = (i\Delta_p - i\Delta_2 - \Gamma_2) \rho_{ca} - i\Omega_p \rho_{cb} + i\Omega_2 \rho_{ba}, \tag{6}$$

Where  $\gamma_1$ ,  $\gamma_2$ ,  $\Gamma_1$  and  $\Gamma_2$  are the decay rates in the system, as shown in Figure 1a and 1b. The Equations (3) and (4) correspond to the water-atom and Equations (5) and (6) belong to the red blood cell.

Chen et al. [5] has shown that the water splitting depends on the rotor angle and magnetic field which can be given by

$$\Delta\nu = \left(1 - \sin^2 \frac{\theta}{2}\right) \Delta\chi\nu_o \tag{7}$$

Where  $\nu_o = \gamma B_o$  and  $\Delta\chi = \chi_w - \chi_c$ . Equation (7) shows that the huge signal splitting  $\Delta\nu = \Delta\chi\nu_o$  can be observed by placing the sample parallel to the applied magnetic field. For the perpendicular case, we would be expecting the small

splitting  $\Delta\nu = \frac{\Delta\chi\nu_o}{2}$ . The splitting at the magic angle can be given by

$$\Delta\nu = \frac{3}{2} \Delta\chi\nu_o \tag{8}$$

Using the proposed models for the water-atom and the red blood cell, the susceptibilities  $\chi_w$  and  $\chi_c$  can be calculated as

$$\chi_w = \frac{i\Gamma_1 + i(\Delta_1 - \Delta_p)}{\gamma_1\Gamma_1 + i\gamma_1\Delta_1 - i\gamma_1\Delta_p - i\Gamma_1\Delta_p + \Delta_1\Delta_p - \Delta_p^2 + \Omega_1^2}, \tag{9}$$

and,

$$\chi_c = \frac{i\Gamma_2 + i(\Delta_2 - \Delta_p)}{\gamma_2\Gamma_2 + i\gamma_2\Delta_2 - i\gamma_2\Delta_p - i\Gamma_2\Delta_p + \Delta_2\Delta_p - \Delta_p^2 + \Omega_2^2}, \tag{10}$$

### RESULTS AND DISCUSSION

Here, we extend the study on the splitting of water peaks theoretically and investigate the influence of the varying magnetic field, varying spinning angle, detunings and varying electric field on the splitting of water peaks which could change the behavior of the proposed water-cell system. Initially, we present a comprehensive theory for the splitting of water peaks which is based on the atomic model that consists of two different cells having different susceptibilities. Further, we study the effect of the strength of the magnetic field, the magic spinning angle, the electric field, and detunings on the splitting of water peaks. We choose the corresponding parameters as  $\gamma_1 = 1\gamma$ ,  $\gamma_2 = 1\gamma$ ,  $\gamma_3 = 1\gamma$ ,  $\Delta_1 = 0\gamma$ ,  $\Gamma_1 = 1.5\gamma$ ,  $\Gamma_2 = 1.4\gamma$ ,  $\Delta_2 = -0.5\gamma$ ,  $\Omega_1 = 2\gamma$ ,  $\Omega_2 = 1.9\gamma$ .

We investigate the effect of varying magnetic field on the splitting of water peaks, as presented in Figure 2. When the magnetic field is low i.e., 0.5 T, even there is a splitting of water peaks as shown by the pink curve in Figure 2. The height of the splitting peaks increases further by varying the magnetic field, for example, we observe a yellow curve for a B=0.8 T, the blue curve for B=0.9 T, respectively. Further, when the magnetic field goes to B=1 T, the height of both splitting peaks increases significantly, showing the large effect of magnetic field on the peaks. Here, all other parameters are kept the same as in the case of the pink curve. Hence, the height of splitting peaks can be controlled to the desired value by controlling the magnetic field.

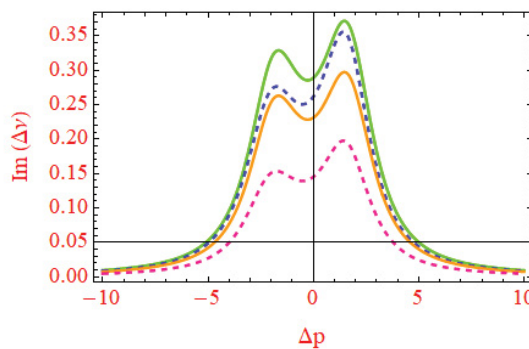


**Figure 2:** Splitting of water peaks versus probe field detunings. Here, we have chosen the following parameters:  $\gamma_1=1\gamma$ ,  $\gamma_2=1\gamma$ ,  $\gamma_3=1\gamma$ ,  $\Gamma_1=1.5\gamma$ ,  $\Gamma_2=1.4\gamma$ ,  $\Delta_1=-0.5\gamma$ ,  $\Omega_1=2\gamma$ ,  $\Omega_2=1.9\gamma$ ,  $\theta=\pi/2$ , B=0.5T, 0.8T, 0.9T and 1T

Next, we monitor the influence on the splitting water peaks by varying the spinning angle of the rotor. The relation between the splitting of water peaks  $\Delta V$  and the rotor angle  $\theta$  is given by Equation (7). Figure 3 presents the effect of varying spinning angle on the splitting of water peaks. The strength of the magnetic field is chosen 1 T and all other parameters are kept constant as in Figure 2. The height of the splitting of water peaks is maximum at zero spinning angle, as shown by the green curve in Figure 3. The height of peaks decreases with increasing the spinning angle as shown by pink, yellow and blue curves in Figure 3 by keeping the spinning angle at  $60^\circ$ ,  $45^\circ$ , and  $30^\circ$  respectively. Hence the spinning angle is another controlling parameter that can be used to achieve the desired height of splitting of water peaks.

Further, we investigate the effect of detunings on the splitting of water peaks. Specifically, we choose the strength of the magnetic field 1 T and spinning angle  $0^\circ$  while keeping other parameters the same as in Figure 2. The splitting of water peaks is observed at different detunings of the cell, i.e.,  $\Delta_2 = -0.5\gamma, -1\gamma, -1.5\gamma$  and  $-2\gamma$ . We notice the enhancement of the right peak and reduction of the left peak by changing detunings, as shown in Figure 4. The detunings is another controlling parameter that can be used to vary the height of the splitting of water peaks.

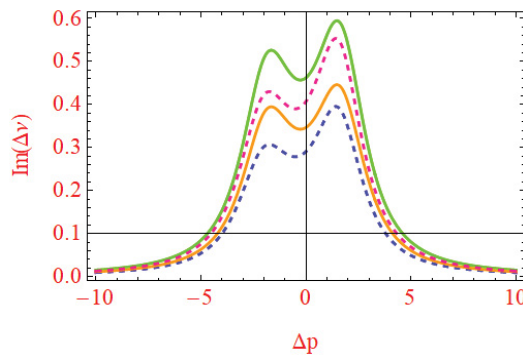


**Figure 3:** Splitting of water peaks varies due to probe field detunings. The parameters are kept as

$$\gamma_1 = 1\gamma, \gamma_2 = 1\gamma, \gamma_3 = 1\gamma, \Gamma_1 = 1.5\gamma, \Gamma_2 = 1.4\gamma, \Delta_1 = -0.5\gamma, \Omega_1 = 2\gamma, \Omega_2 = 1.9\gamma, B = 1T, \theta = 0, \pi / 6, \pi / 4, \pi / 3$$

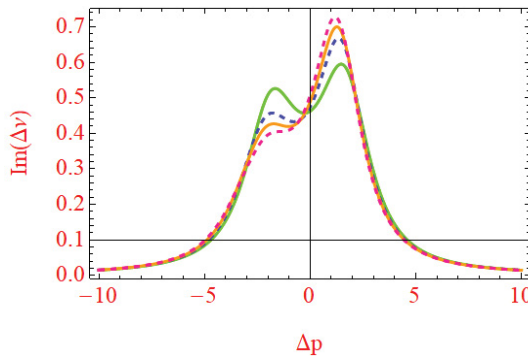


**Figure 4:** Splitting of water peaks with probe field detunings and parameters are kept as

$$\gamma_1 = 1\gamma, \gamma_2 = 1\gamma, \Gamma_1 = 1.5\gamma, \Gamma_2 = 1.4\gamma, \Delta_1 = -0.5\gamma, \Omega_1 = 2\gamma, 2.5\gamma, 3\gamma, 3.2\gamma, \text{ and } \Omega_2 = 3.5\gamma$$

Further, it is also worthy to study the influence of the electric field on the splitting of water peaks. Here we choose different strength of the electric field of the  $\Lambda$ - and cascade  $\Xi$ -type atomic configurations while keeping all other parameters same as in Figure 3. To study the influence of the electric field on the splitting of water peaks, we plot the susceptibility difference with probe detunings. Moreover, we have chosen an electric field in the cascade system to be constant i.e.,  $\Omega_2 = 3.5\gamma$ . In Figure 5, the green plot shows the splitting of water peaks  $\Omega_1 = 2\gamma$ . We observe a strong effect in our system when we keep the electric field up to  $3.2\gamma$  i.e., red curve. Hence, this is obvious from the result that by increasing the strength of the electric field, one can obtain a higher height for the water peaks comparatively to the case of the low electric field. the plots show that the splitting of water decreases with the increase of the electric field at resonance condition i.e.,  $\Delta_p = 0\gamma$ . The electric field could be used as an exciting parameter to vary the height of water peaks.

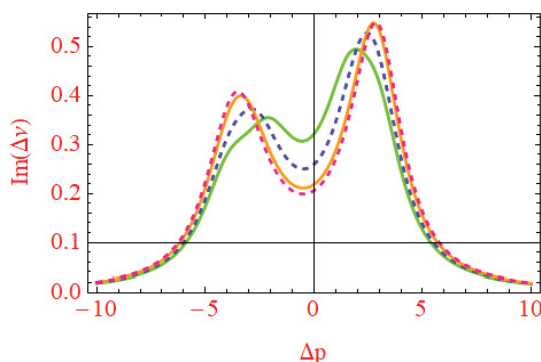


**Figure 5:** Splitting of water peaks with probe field detunings and parameters are kept as

$$\gamma_1 = 1\gamma, \gamma_2 = 1\gamma, \Gamma_1 = 1.5\gamma, \Gamma_2 = 1.4\gamma, \Delta_1 = -0.5\gamma, \Omega_1 = 2\gamma, \Omega_2 = 1.9\gamma, \Delta_2 = 0\gamma, -1\gamma, -1.5\gamma, -2\gamma$$

### CONCLUSION

In this work, we have suggested a scheme for controlling or varying the height of water peaks inside the atomic system. We theoretically investigated the change in splitting of water peaks via varying magnetic field, magic spinning angle, detunings as well as the electric field inside the system. Each atom of the collective molecule consists of three-level-type atomic configuration and we studied the dependency of susceptibility difference on the splitting of levels. A very strong influence on the splitting of water peaks was examined via externally controlled-electric field, magnetic field, magic spinning angle and detunings as well.

### ACKNOWLEDGEMENT

We are thankful to the Higher Education Commission (HEC) of Pakistan for funding this work by the project numbers 2421 and 1414.

### REFERENCES

1. Renault, M., et al., Slow-spinning low-sideband HR-MAS NMR spectroscopy: Delicate analysis of biological samples. *Scientific Reports*, **2013**. 3: p. 3349.
2. Mehring, M., High-resolution NMR in solids, 2nd ed., *Springer*, **1983**.
3. Garroway, A.N., Magic-angle sample spinning of liquids. *J Magn Reson*, **1982**. 49: p. 168-171.
4. Barbara, T.M., Cylindrical demagnetization fields and microprobe design in high-resolution NMR. *J Magn Reson A*, **1994**. 109: p. 265-269.
5. Chen, J.H., et al., Isotropic susceptibility shift under MAS: The origin of the split water resonances in  $^1\text{H}$  MAS NMR spectra of cell suspensions. *Magn Reson Med*, **2003**. 50(3): p. 515-521.
6. Marti, R.W., et al., High-resolution nuclear magnetic resonance spectroscopy of biological tissues using projected magic angle spinning. *Magn Reson Med*, **2005**. 54(2): p. 253-257.
7. Taylor, J.L., et al., High resolution magic angle spinning proton NMR analysis of human prostate tissue with slow spinning rates. *Magn Reson Med*, **2003**. 50: p. 627-632.
8. Wu, C.L., et al., Proton high-resolution magic angle spinning NMR analysis of fresh and previously frozen tissue of human prostate. *Magn Reson Med*, **2003**. 50(6): p. 1307-1311.
9. Chen, J.H., et al., Resolution of creatine and phosphocreatine  $^1\text{H}$  signals in isolated human skeletal muscle using HR-MAS  $^1\text{H}$  NMR. *Magn Reson Med*, **2008**. 59(6): p. 1221-1224.
10. Aime, S., et al., HR-MAS of cells: A "Cellular Water Shift" due to water- protein interactions? *Magn Reson Med*, **2005**. 55: p. 1547-1552.
11. Philp, D.J., Bubb, W.A., and Kuchel, P.W., Chemical shift and magnetic susceptibility contributions to the

- separation of intracellular and supernatant resonances in variable angle spinning NMR spectra of erythrocyte suspensions. *Magn Reson Med*, **2004**. 51: p. 441-444.
12. Scully, M., and Zubairy, M., Quantum Optics, Cambridge University Press, Cambridge. **1997**.
  13. Ali, H., and Ahmed, I., Control of wave propagation and effect of kerr nonlinearity on group index. *Commun Theor Phys*, **2013**. 60(1): p. 87.
  14. Ali, H., and Ahmed, I., The effect of Kerr nonlinearity and doppler broadening on slow light propagation. *Laser Phys*, **2014**. 24(2): p. 025201.
  15. Ali, H., and Ahmed, I., Control of wave propagation via spontaneous generated coherence and Kerr non-linearity. *Commun Theor Phys*, **2014**. 62: p. 410-416.